Doubly differential cross sections of secondary electrons ejected from atomic hydrogen by electron impact

T. W. Shyn
Space Physics Research Laboratory, The University of Michigan, Ann Arbor, Michigan 48109
(Received 18 March 1991; revised manuscript received 13 August 1991)

We have measured the doubly differential cross sections, in angle and energy, of secondary electrons ejected from atomic hydrogen by electron impact. The incident energies used were from 25 to 250 eV. The energy and angular range of secondary electrons measured were from 1.0 eV to one-half of the difference between the incident energy and the ionization potential of hydrogen atom and from 12° to 156°, respectively. Singly differential cross sections and total-ionization cross sections were obtained from the doubly differential cross sections. The present total-ionization cross sections were compared with previous measurements and theoretical results. Discrepancies have been found between the present results and those measurements and theoretical results.

PACS number(s): 34.80.Dp

I. INTRODUCTION

The study of the inelastic electron-atom scattering process is of fundamental importance for the understanding of the physical structure of atoms and molecules and the effects contributing to the collision process. In particular, the ionization of atomic hydrogen by electron impact is of fundamental importance and is the simplest process of atomic physics leading to three free particles in the final state. Also, in general, the more differential in angle and energy the cross section is, the more detailed information can be obtained about the nature of the process.

Experimental measurements of doubly differential cross sections (DDCS) in angle and energy have recently been performed by this author [1–5] as well as by other groups [6–8]. Most of the work has concentrated on elements such as helium and diatomic molecules, but not on atomic hydrogen. However, there were three measurements of the total-ionization cross sections of atomic hydrogen: Fite and Brackmann [9] measured the total ionization by electron impact from near threshold to 1000 eV, Rothe *et al.* [10] measured the cross section from 100 to 750 eV and, recently, Shah, Elliott, and Gilbody [11] measured the total-ionization cross sections in the range 14.6–4000 eV by a pulsed crossed-beam method. On the theoretical side, the best available theoretical calculation of DDCS is based on the plane-wave Born approximation [12,13], which can only be expected to be valid at very high incident energies. The total ionization was calculated by Akerib and Borowitz [14] using the impulse approximation. This calculation shows better agreement with the measurements below 100 eV than do the results of the Born approximation.

This paper presents the results of experiments in which the DDCS of secondary electrons ejected from atomic hydrogen have been measured by electron impact over the angular range of 12° to 156° and the incident energy range of 25 to 250 eV. The measured energies of the secondary electrons were from 1.0 eV to one-half of the difference between the incident energy and ionization potential. This energy range of secondary electrons constitutes the total-ionization cross sections by definition. Most of the contribution to the total-ionization cross section comes from the low-energy side of the secondary-electron energy (<5 eV).

II. APPARATUS AND PROCEDURE

A detailed description of the apparatus used for this work can be found elsewhere [3–5]. Briefly, there are two chambers, upper and lower, which are pumped differentially.

An atomic-hydrogen generator is located in the upper chamber. A beam of atomic hydrogen is generated by a microwave discharge. A neutral beam of mixed atomic and molecular hydrogen emerges through a slit in the discharge device and is collimated by a skimmer before entering the lower chamber where the cross sections are measured. The atomic and the molecular hydrogen in the beam are expected to be mainly in the ground state. The degree of dissociation of hydrogen molecules into atomic hydrogen was very closely monitored using a quadrupole mass spectrometer (UTI 100C) located at the interaction region in the lower chamber. The dissociation rate D was obtained by

$$D = 1 - S^{\text{on}}_{H_2} / S^{\text{off}}_{H_2} , \tag{1}$$

where $S^{\text{on}}_{H_2}$ and $S^{\text{off}}_{H_2}$ are the intensities of the modulated molecular-hydrogen beam at the interaction region when the microwave discharge device is on and off. D was measured to be $(66\pm3)\%$.

In the lower chamber, there is an electron-beam source that consists of an electron gun, a 127° electrostatic energy selector, two electron lens systems, and two beam deflectors. This electron beam can be rotated from $-90°+160°$ continuously. The electron-beam source can produce a current exceeding 10^{-7} A at energies above 10 eV with 80 meV full width at half maximum (FWHM). The half-angle spread of the electron beam was less than $\pm3°$.

TABLE I. DDCS ($d^2\sigma/d\Omega dE$) of secondary electrons ejected from H by 25-eV impact (in units of 10^{-19} cm^2/sr eV). The numbers in parentheses represent extrapolated data points.

	θ (deg)														$\Delta\sigma/\Delta E$
E_s (eV)	12	24	36	48	60	72	84	96	108	120	132	144	156	168	(10^{-17} cm^2/eV)
1.0	24.6	16.8	10.8	7.9	5.4	5.1	4.9	5.4	4.9	6.8	7.2	8.0	9.3	(10.2)	0.93
2.0	14.5	13.7	12.3	8.1	5.5	4.5	3.8	4.6	3.9	5.4	7.3	8.5	9.9	(11.2)	0.85
3.0	14.2	11.7	10.5	9.1	5.4	3.2	3.0	3.2	4.0	4.5	6.5	9.6	10.3	(13.1)	0.78
4.0	16.8	12.0	8.2	4.8	3.4	3.5	3.1	2.9	3.6	3.7	5.4	8.2	9.1	(11.8)	0.66
5.7	14.6	12.7	8.1	3.9	3.5	3.2	3.0	2.7	2.9	3.3	3.4	3.9	4.9	(5.8)	0.54

The detector system, also in the lower chamber, is fixed to the vacuum chamber wall. It has two electron lens systems, an electrostatic energy analyzer, and a channeltron electron multiplier. The energy resolution of the detector system was better than 60 meV (FWHM).

The beam was modulated at an audio frequency ($\approx$150 Hz) by a toothed chopper wheel so that the pure beam signal could be separated from the background by using a phase-sensitive detector. Since the time constant of the present vacuum system for molecular hydrogen is estimated to be longer than 0.2 sec, it is believed, therefore, to make a negligible contribution to the beam signal from the background pressure. The chopping period ($\approx$7 msec) is shorter than the time constant of the vacuum system by more than 30 times.

The modulated neutral beam interacts with an electron beam of fixed energy in the horizontal plane. The scattered and ejected electrons at a given angle from the modulated beam were detected by a channeltron electron multiplier after energy and phase analysis. The measurement was repeated at different angles and secondary-electron energies for a given incident energy.

The absolute DDCS's of atomic hydrogen, $[d^2\sigma_H(E_i,E_s,\theta)/d\Omega dE]$, have been obtained by normalizing to the DDCS's of molecular hydrogen using the following equation,

$$\frac{d^2\sigma_H(E_i,E_s,\theta)}{d\Omega dE}=S_T(E_i,E_s,\theta)/(\sqrt{2}DN) -[(1-D)/\sqrt{2}D]\frac{d^2\sigma_{H_2}(E_i,E_s,\theta)}{d\Omega dE}, \quad (2)$$

where

$$N=S_{H_2}(E_i,E_s,\theta)\Big/\frac{d^2\sigma_{H_2}(E_i,E_s,\theta)}{d\Omega dE}, \quad (3)$$

and $S_T(E_i,E_s,\theta)$ is a total signal from the mixed neutral beam at incident energy E_i, secondary-electron energy E_s, and angle θ. N is a normalization factor against the DDCS of molecular hydrogen, $d^2\sigma_{H_2}(E_i,E_s,\theta)/d\Omega dE$, and $S_{H_2}(E_i,E_s,\theta)$ is the total signal from pure molecular hydrogen at E_i, E_s, and θ (when the dissociation device was off). The DDCS's of the hydrogen molecule measured by the present author [3] were used for the normalization.

III. EXPERIMENTAL RESULTS

We measured absolute doubly differential cross sections of secondary electrons ejected from atomic hydrogen by electron impact. A modulated crossed-beam method was used with incident energies of 25, 50, 75, 100, 150, 200, and 250 eV.

The statistical uncertainty of the present measurement was 5% and the uncertainty in the normalization procedure was 7%. The overall uncertainty of this measurement was about $\pm$20% including the uncertainty in the DDCS of H_2 ($\pm$16%).

Absolute DDCS's and singly differential cross sections (SDCS) for the six incident energies measured are shown in Tables I–VI. The SCDS's were obtained by first extrapolating the DDCS to 180° and then integrating them over solid angles. For large angles, a less-steep dependence on the scattering angle and the sinθ factor in the

TABLE II. DDCS ($d^2\sigma/d\Omega dE$) of secondary electrons ejected from H by 40-eV impact (in units of 10^{-19} cm^2/sr eV). The numbers in parentheses represent extrapolated data points.

	θ (deg)														$\Delta\sigma/\Delta E$
E_s (eV)	12	24	36	48	60	72	84	96	108	120	132	144	156	168	(10^{-17} cm^2/eV)
1.0	26.7	22.7	20.0	13.6	13.3	9.1	6.1	6.1	6.9	6.9	7.9	9.7	10.3	(11.9)	1.31
2.0	20.7	18.4	14.9	12.7	10.6	7.5	5.2	5.3	6.4	7.3	9.3	10.2	10.5	(11.9)	1.17
3.0	13.1	12.3	11.3	9.2	7.1	4.7	4.5	3.9	5.4	6.4	7.5	9.9	10.4	(12.5)	0.91
4.0	12.0	11.5	9.5	6.4	5.6	3.7	2.5	2.6	3.3	3.9	4.4	6.1	6.5	(7.7)	0.64
5.0	9.8	9.1	7.0	4.2	3.3	2.8	2.8	3.0	2.6	3.0	3.5	5.6	6.6	(7.2)	0.52
6.0	6.0	4.9	4.5	3.4	2.8	2.3	2.3	2.2	2.1	2.7	2.9	4.0	4.4	(5.2)	0.39
8.0	5.1	4.9	4.7	3.0	2.6	2.3	2.0	1.6	1.8	1.9	1.9	2.0	2.5	(2.8)	0.31
10.0	4.6	3.8	3.5	2.4	2.1	1.9	1.5	1.3	1.2	1.4	1.5	1.8	2.0	(2.4)	0.24
13.3	4.4	2.8	1.9	1.7	1.5	1.2	1.0	0.9	1.1	1.0	1.0	1.1	1.4	(1.6)	0.17

TABLE III. DDCS ($d^2\sigma/d\Omega dE$) of secondary electrons ejected from H by 60-eV impact (in units of 10^{-19} cm^2/sr eV). The numbers in parentheses represent extrapolated data points.

	θ (deg)														$\Delta\sigma/\Delta E$
E_s (eV)	12	24	36	48	60	72	84	96	108	120	132	144	156	168	(10^{-17} cm^2/eV)
1.0	34.9	23.1	19.6	15.3	11.4	8.3	7.2	6.7	8.8	8.0	8.1	7.9	9.9	(10.7)	1.35
2.0	24.4	21.4	16.0	13.2	8.4	7.2	5.7	6.1	7.2	7.4	7.3	7.4	8.5	(8.6)	1.19
3.0	18.1	17.5	14.9	9.2	8.1	5.8	5.8	4.7	4.7	4.9	5.7	6.7	8.1	(9.2)	0.94
4.0	13.9	12.6	11.1	7.7	5.8	4.0	3.7	4.3	4.0	4.5	4.7	5.0	6.4	(7.4)	0.72
5.0	11.0	9.8	8.0	5.8	3.7	3.2	3.2	2.5	2.4	3.0	3.4	3.7	4.5	(5.1)	0.55
6.0	8.9	8.3	6.4	4.7	3.8	2.8	2.2	2.1	2.0	2.6	2.9	3.5	4.4	(5.2)	0.45
8.0	8.2	6.8	5.8	3.3	2.8	2.4	2.0	1.7	1.6	2.0	2.3	2.5	3.6	(4.2)	0.36
10	7.7	5.6	4.0	3.2	2.6	2.5	1.9	1.6	1.5	1.8	2.2	2.3	2.3	(2.6)	0.32
12	5.2	3.9	3.6	2.6	2.4	1.5	1.2	1.1	0.97	1.1	1.2	1.3	1.4	(1.5)	0.22
15	4.5	3.5	3.2	2.7	1.9	1.3	1.1	0.77	0.86	0.83	0.93	1.1	1.1	(1.2)	0.19
20	4.1	2.3	1.8	1.2	1.1	0.65	0.63	0.57	0.43	0.55	0.59	0.65	0.85	(0.96)	0.12
23.3	4.4	2.9	2.1	1.1	0.63	0.54	0.40	0.37	0.37	0.34	0.43	0.49	0.61	(0.71)	0.10

calculation of the SDCS leads one to expect a small uncertainty. The total-ionization cross sections were obtained by integrating the SDCS's over a secondary-electron-energy *range* and are shown in Table VII along with the measurements of Fite and Brackmann, those of Rothe *et al.*, and those of Shah, Elliott, and Gilbody.

Figure 1 shows the DDCS of secondary-electron energy 2.0 eV at 25-eV incident energy and 15-eV secondary-electron energy at 100-eV impact. These show a minimum near 90°. All angular distributions of secondary electrons have nearly the same shape. The general trend is that the backward scattering becomes smaller than the forward as the secondary-electron energy increases. A small bump for 100-eV impact that is commonly referred to as the "binary collision peak" near 60° is caused by the conservation of energy and the momentum of the colliding system. A similar trend in the DDCS continues at impact energies up to 250 eV.

Figure 2 shows the SDCS of 25-, 60-, and 100-eV incident energy. At 25 eV, the slope is mostly flat over the secondary-electron energy range. At 60 eV, the largest SDCS was shown and a relatively sharp decrease was noticed as the secondary-electron energy increases. The SDCS at 100 eV is reduced uniformly from those of 60-eV impact in the secondary-electron energy region.

Figure 3 is the same as Fig. 2 except for 150- and 250-eV impact. The slope of the SDCS curve becomes steeper as the incident energy increases.

The Platzman plot of the present results is shown in Fig. 4. A detailed description and the meaning of the Platzman plot can be found elsewhere [3]. Briefly, the abscissa is $\mathcal{R}/E$ ($\mathcal{R}=13.6$ eV) where E is the energy transfer. This amplifies the effects at the low-energy side. The ordinate Y is the cross section in units of the Ruther-

TABLE IV. DDCS ($d^2\sigma/d\Omega dE$) of secondary electrons ejected from H by 100-eV impact (in units of 10^{-19} cm^2/sr eV). The numbers in parentheses represent extrapolated data points.

	θ (deg)														$\Delta\sigma/\Delta E$
E_s (eV)	12	24	36	48	60	72	84	96	108	120	132	144	156	168	(10^{-17} cm^2/eV)
1.0	26.2	25.4	19.3	11.4	6.2	6.6	7.0	6.1	6.3	5.5	5.0	5.6	5.7	(5.8)	1.08
2.0	18.4	16.2	14.4	11.6	5.6	5.2	5.6	5.8	5.3	5.2	4.1	3.8	4.1	(4.0)	0.86
3.0	14.8	11.2	10.9	10.8	6.2	5.0	4.4	4.2	3.4	3.7	3.2	2.9	3.3	(3.2)	0.70
4.0	12.8	11.6	9.1	6.9	4.0	3.0	2.8	2.8	2.6	2.8	2.6	2.2	2.5	(2.4)	0.52
5.0	8.8	7.5	6.6	5.4	3.2	2.2	2.2	2.4	2.3	2.3	2.3	2.4	2.8	(2.9)	0.41
6.0	7.7	6.2	6.3	3.9	3.2	2.6	2.4	2.1	1.8	1.8	2.1	2.1	2.5	(2.7)	0.37
8.0	6.3	4.1	3.0	3.2	2.5	1.5	1.4	1.4	1.6	1.7	1.6	1.7	1.9	(2.0)	0.26
10	4.7	3.6	3.1	2.9	2.5	1.3	0.85	0.76	0.84	1.0	1.1	1.3	1.5	(1.8)	0.21
12	3.6	2.8	2.3	2.3	1.7	1.3	0.98	0.78	0.82	0.85	1.0	1.5	1.6	(1.6)	0.15
15	2.5	2.3	1.6	1.5	1.2	0.82	0.61	0.59	0.62	0.70	0.73	0.78	0.82	(0.90)	0.12
20	1.4	1.1	1.2	1.0	0.74	0.52	0.45	0.37	0.36	0.34	0.35	0.36	0.42	(0.46)	0.072
25	0.95	0.61	0.61	0.64	0.60	0.39	0.29	0.26	0.26	0.25	0.26	0.30	0.34	(0.38)	0.050
30	0.98	0.73	0.72	0.63	0.46	0.30	0.20	0.14	0.15	0.18	0.18	0.19	0.22	(0.23)	0.041
35	0.89	0.52	0.55	0.42	0.31	0.20	0.13	0.13	0.13	0.13	0.13	0.13	0.15	(0.16)	0.030
40	0.76	0.63	0.51	0.39	0.31	0.18	0.16	0.11	0.10	0.12	0.12	0.12	0.14	(0.15)	0.029
43.3	0.74	0.68	0.43	0.34	0.22	0.15	0.11	0.10	0.09	0.10	0.12	0.12	0.14	(0.15)	0.025

TABLE V. DDCS ($d^2\sigma/d\Omega dE$) of secondary electrons ejected from H by 150-eV impact (in units of 10^{-20} cm^2/sr eV). The numbers in parentheses represent extrapolated data points.

	θ (deg)														$\Delta\sigma/\Delta E$
E_s (eV)	12	24	36	48	60	72	84	96	108	120	132	144	156	168	(10^{-18} cm^2/eV)
1.0	176	157	131	111	67	58	54	48	47	49	52	54	62	(68)	8.74
2.0	159	131	116	85	60	55	47	39	39	41	42	44	53	(54)	7.45
3.0	121	112	94	80	56	42	35	32	39	36	34	36	39	(42)	6.23
4.0	103	99	87	66	54	33	29	25	26	25	25	26	31	(33)	5.09
5.0	96	85	78	56	38	28	24	25	24	24	25	24	25	(26)	4.41
6.0	82	76	62	39	29	22	18	18	18	17	20	20	21	(22)	3.50
8.0	67	50	39	29	25	18	15	15	14	15	16	15	15	(16)	2.66
10	36	34	29	22	19	13	8.8	8.2	9.6	8.5	8.8	10	12	(13)	1.82
12	26	21	19	13	13	8.2	7.1	6.8	6.5	7.1	7.6	7.5	9.0	(9.0)	1.29
15	18	16	15	11	11	6.8	5.9	4.4	4.3	4.6	4.9	5.1	6.5	(7.0)	0.91
20	11	9.3	8.5	5.1	4.1	3.7	2.9	2.7	2.8	2.3	2.4	2.9	3.7	(4.6)	0.50
25	7.7	7.0	6.3	4.4	3.5	2.6	2.4	1.7	1.7	1.8	2.0	2.0	2.4	(2.6)	0.37
30	5.8	4.1	3.4	3.3	2.8	2.3	1.8	1.5	1.2	1.2	1.5	1.5	1.7	(1.8)	0.27
35	3.0	3.0	3.0	2.5	2.1	1.1	0.84	0.84	0.91	0.84	0.91	0.91	1.1	(1.1)	0.18
40	2.0	1.8	1.7	1.6	1.1	0.84	0.68	0.71	0.76	0.84	0.79	0.79	1.0	(1.1)	0.12
50	2.1	1.9	1.9	1.5	1.0	0.49	0.47	0.52	0.49	0.44	0.47	0.36	0.40	(0.4)	0.10
60	2.0	1.7	1.5	1.1	0.84	0.52	0.50	0.47	0.44	0.47	0.38	0.39	0.43	(0.5)	0.08
68.3	2.4	2.1	1.4	0.91	0.74	0.41	0.40	0.33	0.36	0.36	0.35	0.36	0.40	(0.4)	0.08

TABLE VI. DDCS ($d^2\sigma/d\Omega dE$) of secondary electrons ejected from H by 250-eV impact (in units of 10^{-20} cm^2/sr eV). The numbers in parentheses represent extrapolated data points.

	θ (deg)														$\Delta\sigma/\Delta E$
E_s (eV)	12	24	36	48	60	72	84	96	108	120	132	144	156	168	(10^{-18} cm^2/eV)
1.0	154	146	93	51	45	33	34	30	30	30	38	44	51	(59)	6.08
2.0	116	105	77	62	42	30	26	28	27	23	23	28	33	(38)	4.94
3.0	102	90	84	55	35	27	23	22	21	19	18	19	21	(22)	4.18
4.0	97	81	62	39	32	22	21	21	20	15	14	15	18	(19)	3.50
5.0	75	66	62	35	30	19	17	15	15	14	13	14	16	(17)	3.12
6.0	63	55	42	24	19	16	13	13	13	13	12	14	15	(16)	2.43
8.0	37	35	28	21	11	11	9.1	8.4	9.1	11	10	9.1	11	(12)	1.67
10	40	35	25	14	11	9.1	7.6	7.6	5.5	5.6	5.3	6.1	7.1	(7.6)	1.37
12	28	23	18	13	11	7.6	6.4	5.0	5.8	5.0	5.2	4.9	6.0	(6.2)	1.06
15	21	15	14	11	7.6	6.1	3.8	3.0	2.9	3.0	3.5	3.5	3.8	(4.6)	0.76
20	12	9.1	7.6	5.3	4.6	2.7	2.3	2.1	2.1	2.6	2.7	2.4	3.0	(3.0)	0.46
25	7.6	5.9	4.6	3.3	3.2	2.6	2.0	1.7	1.8	2.0	1.8	1.5	1.7	(1.7)	0.33
30	4.3	3.8	3.4	2.8	2.1	1.5	1.1	1.3	1.3	1.3	1.4	1.5	1.5	(1.6)	0.23
40	2.7	2.2	1.8	1.4	1.3	0.91	0.73	0.73	0.68	0.50	0.55	0.50	0.55	(0.55)	0.11
50	2.3	1.8	1.3	0.99	0.91	0.59	0.48	0.47	0.43	0.43	0.40	0.53	0.61	(0.63)	0.09
65	1.1	0.99	0.76	0.60	0.33	0.25	0.23	0.27	0.27	0.27	0.27	0.30	0.32	(0.33)	0.05
80	0.76	0.65	0.38	0.30	0.25	0.17	0.19	0.19	0.19	0.17	0.18	0.18	0.21	(0.22)	0.03
100	0.55	0.43	0.40	0.27	0.24	0.16	0.17	0.14	0.14	0.18	0.19	0.25	0.27	(0.30)	0.03
118.3	0.67	0.55	0.49	0.30	0.23	0.17	0.14	0.16	0.14	0.14	0.14	0.18	0.21	(0.24)	0.02

TABLE VII. Total-ionization cross section of H atom (in units of 10^{-17} cm^2).

E_i (eV)	Present results	Fite and Brackman	Rothe *et al.*	Shah, Elliott, and Gilbody
25	4.2	4.4		4.30
40	6.7	6.6		5.78
60	8.7	7.2		6.13
100	7.1	6.4	4.8	5.40
150	6.2	5.3	4.3	4.62
200			3.6	3.98
250	4.7	3.9	3.1	3.43
300			2.6	2.92

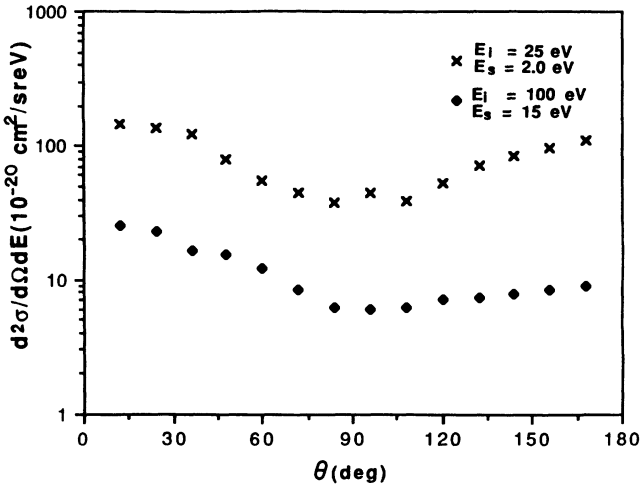

FIG. 1. DDCS of secondary-electron energy (E_s) 2.0 eV ejected from hydrogen atom by 25-eV electron impact (E_i) and 15-eV secondary-electron energy and 100-eV impact energy. Dots are extrapolated data points.

ford cross section of a free electron. The shape of the Platzman plot for electron-impact ionization resembles that of photoionization at much higher incident energies than the ionization potential. The present results show increasing values as the secondary-electron energy decreases for all incident energies, except at 25-eV impact. The dips at $\mathcal{R}/E \approx 2$ may represent the electron-exchange effect.

Finally, Fig. 5 shows the present results of the total-ionization cross sections along with the results of measurements by Fite and Brackmann, Rothe *et al.*, and Shah, Elliott, and Gilbody. The results of the Born approximation and those of Akerib and Borowitz are also included. The results of Fite and Brackmann agree with

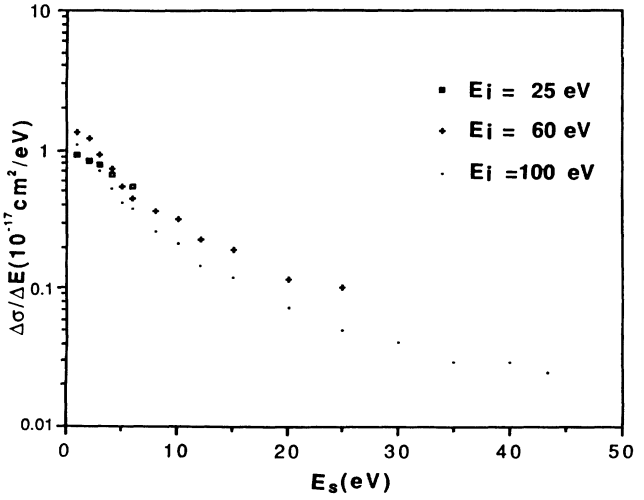

FIG. 2. SDCS ($\Delta\sigma/\Delta E$) at 25-, 60-, and 100-eV impact on hydrogen atoms.

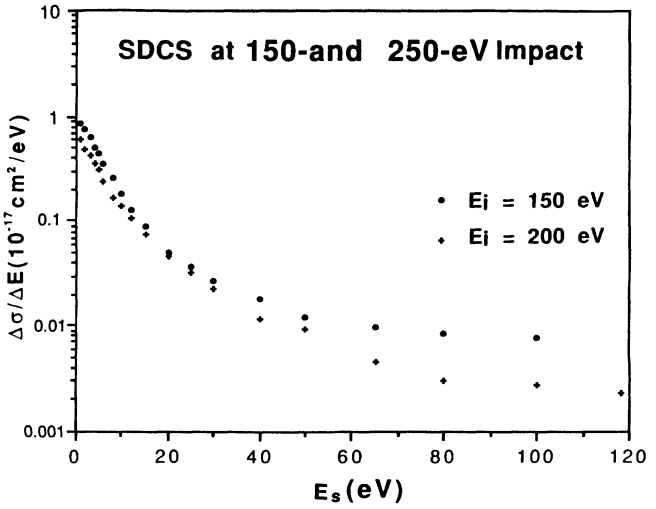

FIG. 3. Same as Fig. 3, except for 150- and 250-eV impact.

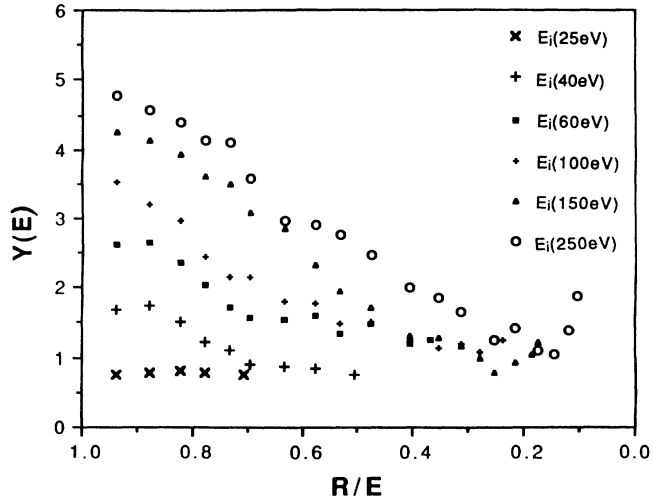

FIG. 4. Platzman plot of secondary electrons ejected from hydrogen atom by electron impact at 25, 40, 60, 100, 150, and 250 eV.

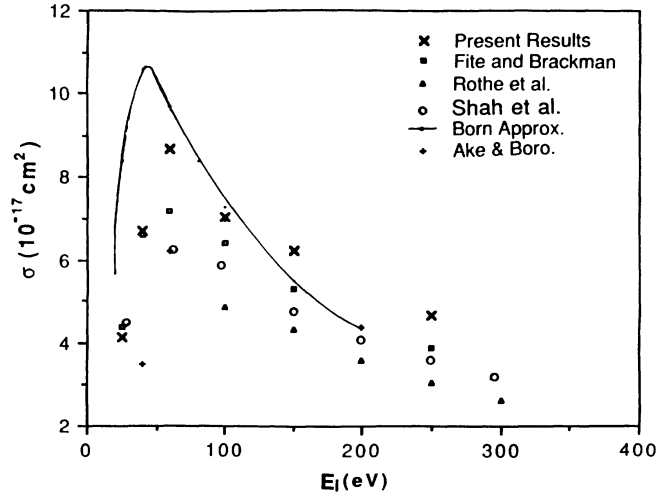

FIG. 5. Total-ionization cross sections of hydrogen atom by electron impact along with those of Fite and Brackmann, Rothe *et al.*, Shah, Elliott, and Gilbody, and the results of the Born approximation and the impulse approximation.

the present results very well below 50 eV, but their values are smaller than the present results by approximately 20%. The results of Rothe *et al.* are smaller than the present results by a factor of approximately 2. The results of Shah, Elliott, and Gilbody are, in general, smaller than the present results by about 25%, except at low energies. The Born approximation predicts cross sections below 100 eV that are about 20% larger than the present results, while above 100 eV the prediction is about 20% smaller than the present results. The impulse approximation results show smaller values than the present results over all energies.

ACKNOWLEDGMENT

This work was supported by NSF Grant Nos. PHY-8700430 and PHY-9010886.

[1] T. W. Shyn and W. E. Sharp, Phys. Rev. A **19**, 557 (1979).
[2] T. W. Shyn and W. E. Sharp, Phys. Rev. A **20**, 2332 (1979).
[3] T. W. Shyn, W. E. Sharp, and Y.-K. Kim, Phys. Rev. A **24**, 79 (1981).
[4] T. W. Shyn, Phys. Rev. A **27**, 2388 (1983).
[5] T. W. Shyn and W. E. Sharp, Phys. Rev. A **43**, 2300 (1991).
[6] C. B. Opal, E. C. Beaty, and W. K. Peterson, Data Nucl. Data Tables **4**, 209 (1972).
[7] E. C. Beaty, Radiat. Res. **64**, 70 (1975).
[8] M. E. Rudd and R. D. DuBois, Phys. Rev. A **16**, 26 (1977).
[9] W. L. Fite and R. T. Brackmann, Phys. Rev. **112**, 1141 (1958).
[10] E. W. Rothe, L. L. Marino, R. H. Neynaber, and S. M. Trujillo, Phys. Rev. **125**, 582 (1962).
[11] M. B. Shah, D. S. Elliott, and H. B. Gilbody, J. Phys. B **20**, 3501 (1987).
[12] H. S. W. Massey and C. B. O. Mohr, Proc. R. Soc. London, Ser. A **140**, 613 (1933).
[13] R. McCarrol, Proc. Phys. Soc. London, Ser. A **70**, 460 (1957).
[14] R. Akerib and S. Borowitz, Phys. Rev. **122**, 1177 (1961).